Tumor angiogenesis suppression by α-eleostearic acid, a linolenic acid isomer with a conjugated triene system, via peroxisome proliferator-activated receptor γ

Tsuyoshi Tsuzuki* and Yuki Kawakami[1]

Laboratory of Biodynamic Chemistry, School of Food, Agricultural and Environment Sciences, Miyagi University, Sendai 982-0215, Japan and [1]Department of Nutritional Science, Faculty of Health and Welfare Science, Okayama Prefectural University, 111 Kuboki, Soja, Okayama 719-1197, Japan

*To whom correspondence should be addressed. Tel: +81 22 245 1382; Fax: +81 22 245 1534;
Email: tsuduki@myu.ac.jp

We have shown previously that α-eleostearic acid (ESA), a linolenic acid isomer with a conjugated triene system, suppresses tumor growth *in vivo*. In our earlier study, blood vessels were observed at the tumor surface in control mice, whereas in ESA-treated mice no such vessels were observed and the inner part of the tumor was discolored. These observations suggested that ESA might suppress cancer cell growth through malnutrition via a suppressive effect on tumor angiogenesis. In the current study, the antiangiogenic effects of ESA were investigated *in vivo* and *in vitro*. Tumor cell-induced vessel formation was clearly suppressed in mice orally administered ESA at doses of 50 and 100 mg/kg/day in a dose-dependent manner. ESA also inhibited the formation of capillary-like networks by human umbilical vein endothelial cells (HUVEC) and moderately inhibited HUVEC proliferation and migration in a dose-dependent manner. The mechanism by which ESA inhibited angiogenesis was through suppression of the expression of vascular endothelial growth factor receptors 1 and 2, activation of peroxisome proliferator-activated receptor γ (PPARγ) and induction of apoptosis in HUVEC. We thus demonstrated that, like troglitazone, ESA is a PPARγ ligand and that it activates PPARγ, induces apoptosis in HUVEC and inhibits angiogenesis. Our findings suggest that ESA has potential use as a therapeutic dietary supplement and medicine for minimizing tumor angiogenesis.

Introduction

Conjugated fatty acid is a generic term for fatty acids with conjugated double-bond systems, as exemplified by conjugated linoleic acid (CLA) (1). Several CLA isomers exist as a result of positional and geometric isomerism of the conjugated double bonds, and the major naturally existing CLA isomer is referred to as 9Z11E-18:2 (1). CLA has been shown to be effective at inhibiting carcinogenesis in multiple systems and at several levels, including initiation (2,3), promotion (4), progression (5) and metastasis (6). These activities of CLA are associated with the conjugated double-bond systems in the molecules.

CLA is found naturally and is especially present in ruminant fats such as beef tallow and milk fat (1). However, it constitutes ~1% of these foodstuffs, which does not allow natural fats to be used as health-promoting foods containing CLA. Therefore, at present, oils that include CLA are prepared by alkali isomerization of vegetable oils such as safflower oil and are marketed as health supplements (7,8). In addition to CLA, many other conjugated fatty acids occur

naturally in plant seeds and marine algae (9–11). Tung and bitter gourd seed oils contain conjugated triene fatty acids such as α-eleostearic acid (ESA, 9Z11E13E-18:3) at concentrations of 60–80% (9). The physiological function of conjugated fatty acids other than CLA is also of interest, and we have described previously the properties of these fatty acids (12–19).

In Okinawa, a region inhabited by the longest living people in Japan, which is in itself one of the leading countries in the world in terms of life expectancy, people often eat bitter gourds (*Momordica charantia*), the seed oil of which contains 60% ESA, a linolenic acid isomer, and the flesh of which contains a small amount of ESA. We are particularly interested in seed oils containing ESA, which is the only conjugated fatty acid that can be prepared from natural sources in bulk, and have shown previously that ESA has a stronger antitumor effect than CLA *in vitro* and *in vivo* (20). In studies in which we transplanted DLD-1 human colorectal adenocarcinoma cells into nude mice and compared tumor growth between ESA-fed mice and CLA-fed or α-linolenic acid (LNA)-fed mice, ESA had a stronger *in vivo* antitumor effect than CLA and LNA. In addition, blood vessels were observed at the tumor surface in control mice, but not in mice that had received CLA or ESA; furthermore, the inner part of the tumor was discolored in the CLA- and ESA-fed mice. These results suggested that tumor angiogenesis is suppressed by CLA, as also reported by others (21,22). The effects of CLA and ESA might be due to the suppression of cancer cell growth through malnutrition, and it is probably that each has a suppressive effect on tumor angiogenesis. The effect of ESA on angiogenesis has not previously been examined, and we therefore investigated this possible antiangiogenic effect as a novel physiological function of ESA.

Antiangiogenic therapy is an established strategy for cancer prevention (23), and we have described previously the antiangiogenic properties of vitamin E (tocotrienol) and polyunsaturated fatty acids (24–26). Angiogenesis involves a series of steps, including endothelial cell activation and breakdown of the basement membrane, followed by migration, proliferation and tube formation of endothelial cells (27). The purpose of this study was to obtain direct evidence for the effects of ESA on angiogenesis both *in vivo* and *in vitro*. We evaluated the antiangiogenic effect of ESA *in vivo* using a mouse dorsal air sac assay and investigated the effect of ESA on the key steps of angiogenesis *in vitro* using human umbilical vein endothelial cells (HUVEC). Peroxisome proliferator-activated receptor γ (PPARγ) ligands have also been implicated in the modulation of angiogenesis (28–31). PPARγ are members of the nuclear hormone receptor superfamily and induce transcriptional activation of specific genes by binding to specific DNA sequences (32). PPARγ ligands include polyunsaturated fatty acids, several prostanoids such as prostaglandin J2, a variety of non-steroidal antiinflammatory drugs and a class of oral antidiabetic agents (33). We therefore, examined the effect of ESA on angiogenesis via PPARγ.

Materials and methods

Materials

Tung oil (the triacylglycerol form of ESA) and CLA-TG (the triacylglycerol form of CLA prepared from high-linoleic safflower oil) were kindly provided by The Nisshin OilliO Group (Tokyo, Japan). Sodium methoxide/methanol (1 M) solutions were purchased from Wako Pure Chemicals Industries (Osaka, Japan). RPMI 1640 medium (containing 0.3 mg/ml L-glutamine and 2.0 mg/ml sodium bicarbonate), linoleic acid (LA, 18:2, n-6), LNA (18:3, n-3), eicosapentaenoic acid (20:5, n-3) and docosahexaenoic acid (22:6, n-3) were obtained from Sigma (St Louis, MO). Fetal bovine serum (FBS) was purchased from Dainippon Pharmaceutical (Osaka, Japan). Penicillin and streptomycin were from Gibco BRL (Rockville, MD). 9Z11E-CLA (9Z11E, 98% purity), 10E12Z-CLA (10E12Z, 98% purity), troglitazone (PPARγ agonist) and

Abbreviations: CLA, conjugated linoleic acid; CLA-TG, the triacylglycerol form of CLA prepared from high-linoleic safflower oil; ESA, α-eleostearic acid; FBS, fetal bovine serum; GW, GW9662; HUVEC, human umbilical vein endothelial cells; LA, linoleic acid; LNA, α-linolenic acid; RT–PCR, reverse transcriptase polymerase chain reaction; PPARγ, peroxisome proliferator-activated receptor γ; VEGF, vascular endothelial growth factor; VEGF-R1, VEGF receptor 1; VEGF-R2, VEGF receptor 2; WST-1, 4-[3-(4-iodophenyl)-2-(4-nitrophenyl)-2H-5-tetrazolio]-1,3-benzene disulfonate sodium salt.

GW9662 (GW, PPARγ antagonist) were obtained from Cayman Chemical Co. (Ann Arbor, MI). ESA (98% purity) was obtained from Larodan Fine Chemicals (Malmö, Sweden).

Animals and cells

Animal experiments were approved by the Miyagi University Animal Policy committee and mice were maintained according to the Miyagi University guidelines for the care and use of laboratory animals, as described previously (20,26). Four-week-old male ICR mice were obtained from CLEA (Tokyo, Japan) and housed in cages maintained at $23 \pm 1°C$ with a 12 h light:dark cycle. They were acclimatized with laboratory rodent chow and water for 1 week. Human colorectal adenocarcinoma cells (DLD-1) were obtained from the Cell Resource Center for Biomedical Research at Tohoku University School of Medicine (Sendai, Japan) and maintained in Roswell Park Memorial Institute 1640 medium supplemented with 10% FBS, 100 units/ml penicillin and 100 μg/ml streptomycin at 37°C in a humidified atmosphere of 5% CO_2, as described previously (20,34). HUVEC were purchased from Iwaki (Tokyo, Japan). Cells were cultured in HuMedia-EG2™ growth medium (Kurabo, Osaka, Japan) and grown at 37°C in a humidified atmosphere of 5% CO_2 in air, as described previously (25,35). HuMedia-EG2™ medium consists of base medium (HuMedia-EB2™) supplemented with 2% FBS, 0.5 mg/l human epidermal growth factor, 2 mg/l human basic fibroblast growth factor, 5 g/l insulin, 50 g/l gentamicin and 50 mg/l amphotericin B. Tightly confluent monolayers of HUVEC of passage 2–6 were used in the experiments.

Fatty acid composition of CLA-TG and tung oil

CLA-TG or tung oil with a known amount of heptadecanoic acid (17:0, Sigma) as an internal standard was methylated by the addition of sodium methoxide/methanol for 5 min at room temperature, as described previously (20,36,37). The fatty acid composition of the tung oil that was orally administered to mice was 2.3% palmitic acid (16:0), 3.0% stearic acid (18:0), 11.3% oleic acid (18:1, n-9), 1.4% LA (18:2, n-6), 78.6% ESA (9Z11E13E-18:3) and 3.4% others (wt/wt). CLA was not detected in tung oil. The fatty acid composition of the CLA-TG that was orally administered to mice was 5.3% palmitic acid (16:0), 2.9% stearic acid (18:0), 10.0% oleic acid (18:1, n-9), 0.9% LA (18:2, n-6), 38.8% 9Z11E-CLA (9Z11E-18:2), 39.5% 10E12Z-CLA (10E12Z-18:2) and 2.6% others (wt/wt). Total CLA was 78.3%. Test oils for the animal studies were prepared based on these data.

Mouse dorsal air sac assay (in vivo study of angiogenesis)

The effect of ESA on tumor cell-induced angiogenesis *in vivo* was evaluated by mouse dorsal air sac assay, as described previously (26,38). DLD-1 cells (5×10^7 cells) were suspended in 0.2 ml of phosphate-buffered saline. A chamber ring (Millipore, MA) was injected with the cell suspension and subsequently packed with a filter (0.45 μm pore size). The chamber filled with DLD-1 cells was surgically implanted into a subcutaneous dorsal air sac produced by pre-injecting 10 ml air in an ICR mouse. One day after the operation, mice were randomly divided into five groups ($n = 12$). Control ($-$ or $+$) groups received chambers containing phosphate-buffered saline ($-$) or DLD-1 cells ($+$) and were treated with corn oil (ICN Biomedicals, Aurora, OH) by gavage. The triacylglycerol form of ESA and CLA-TG groups were fed with ESA (50 or 100 mg/kg body wt) or CLA (500 mg/kg body wt) by gavage using corn oil as the vehicle. Each mouse received test oil and vehicle (2 ml/kg body wt) once a day for 7 days. After the feeding period, mice were killed under sodium pentobarbital anesthesia and their skins were removed. The skins were photographed and the lengths of all blood vessels within the area attached to the chamber were measured using Adobe Photoshop version 5.5 (Adobe Systems, San Jose, CA).

Tube formation

In vitro angiogenesis assays were performed using an Angiogenesis Kit (Kurabo), according to the manufacturer's instructions, and the formation of capillary-like structures composed of HUVEC cocultured with human diploid fibroblasts was observed, as described previously (25,35). The medium, containing vascular endothelial growth factor (VEGF) (final 10 ng/ml; Kurabo) with various concentrations of ESA (5, 10 or 20 μM), 9Z11E-CLA (100 or 200 μM) or 10E12Z-CLA (100 or 200 μM) was exchanged on days 4, 7 and 9, and the cells were washed and directly fixed with 70% ice-cold ethanol for 30 min in the wells after 11 days of culture. The fixed cells were serially incubated with 1% bovine serum albumin in buffer, mouse monoclonal antibody against human CD31 (Kurabo), alkaline phosphatase-conjugated goat anti-mouse IgG (Kurabo) and BCIP/NBT (violet, Kurabo) and washed and photographed. The images were analyzed using Angiogenesis Image Analyzer software (Kurabo) to measure the gross area of CD31-positive tubes (the area occupied by endothelial tubes) in cultures. Data are presented as percentages in relation to the area occupied by endothelial tubes in untreated cultures. In addition, to examine the relation between PPARγ ligand and angiogenesis,

HUVEC were pretreated without or with the PPARγ antagonist GW (10 μM) for 1 h before ESA (20 μM) or troglitazone (10 μM) treatment and exposed ESA or troglitazone for 4 days in HuMedia-EG2™ medium containing VEGF (10 ng/ml). After treatment, tube formation was evaluated like the above mentioned.

Cell migration

Cell migration was evaluated by the Chemicon QCM 96-well Migration Assay kit (Chemicon International, CA) using Boyden Chamber, according to manufacturer instructions. In brief, HUVEC after 24 h incubation in starvation conditions were transferred (2×10^4 cells per well) to each of the 96 wells of the upper chamber in FBS-free HuMedia-EG2™ medium. HuMedia-EG2™ medium with VEGF (10 ng/ml) containing ESA or CLA at various concentrations was placed into the lower wells of the chamber and covered by the membrane. A growth factor-free medium was used as a negative control [control ($-$)], and VEGF was used as a positive control [control ($+$)]. The chambers were then incubated for 12 h at 37°C. Migrating cells were detached, stained and lysed. The relative fluorescent units were determined by fluorescent enzyme-linked immunosorbent assay reader (GENios, Tecan Japan, Kawasaki, Japan) at 480/520 nm.

Cell proliferation

HUVEC at 90% confluency were trypsinized, transferred to 96-well plates (2000 cells per well) and preincubated in HuMedia-EG2™ medium for 24 h. The culture medium was then changed to medium only or to medium containing VEGF (10 ng/ml) and ESA or CLA at various concentrations and incubated for 24 h. At the end of this period, viable cell numbers were estimated using the 4-[3-(4-iodophenyl)-2-(4-nitrophenyl)-2H-5-tetrazolio]-1,3-benzene disulfonate sodium salt (WST-1) assay, as described previously (25,35). WST-1 is a tetrazolium salt that is converted into the soluble formazan salt by succinate-tetrazolium reductase in the respiratory chain of active mitochondria of proliferating viable cells. The amount of formazan produced is directly proportional to the number of viable cells. Briefly, 10 μl of WST-1 solution (Dojindo, Kumamoto, Japan) was added to each well and incubated at 37°C for 3 h, after which the absorbance of the culture medium at 450 nm was measured using a microplate reader (GENios).

Western blot analysis

HUVEC were examined for the expression of VEGF receptor 1 (VEGF-R1, also known as Flt1) and VEGF receptor 2 (VEGF-R2, also known as KDR/Flk-1) proteins. Cells incubated for 24 h after treatment without or with VEGF (10 ng/ml) and ESA (20 μM) were compared with unexposed cells using western blotting. Immunoblotting was performed as described previously (34). Briefly, cell lysates were prepared and aliquots of each (50 μg of protein) were run on 12% sodium dodecyl sulfate/polyacrylamide gels and blotted onto nitrocellulose membrane (Hybond-p PVDF Membrane, Amersham Biosciences, Piscataway, NJ). Membranes were probed with anti-VEGF-R1, anti-VEGF-R2 and anti-β-actin antibodies (Sigma). The membrane was treated with peroxidase-conjugated goat anti-rabbit IgG antiserum (Dako, Glostrup, Denmark), and immobilized antigens were detected by an enhanced chemiluminescence method using an ECL western blotting detection kit (Amersham Biosciences). The results were visualized using the Dolphin-Chemi (Kurabo) and quantified with Dolphin-1D (Kurabo).

Real-time quantitative reverse transcriptase–polymerase chain reaction assay

For real-time quantitative reverse transcriptase–polymerase chain reaction (RT–PCR) assay, total RNA was extracted from ESA-treated HUVEC (1×10^6 cells) using a commercial kit (RNeasy Mini Kit, Qiagen, Valencia, CA), as described previously (20,25,34). ESA was prepared to a final concentration of 20 μM in HuMedia-EG2™ medium containing VEGF (10 ng/ml). Total RNA was eluted with 30 μl RNase-free water and stored at –80°C until use. The amount of total RNA was determined spectrophotometrically at 260 and 280 nm. RNA integrity was confirmed by visualizing intact 28S and 18S ribosomal RNA on a formaldehyde denaturing agarose gel. Expression levels of VEGF-R1, VEGF-R2, PPARγ, Bax (known as an apoptosis-inducing factor) and Bcl-2 (known as an apoptosis-suppressing factor) mRNA in HUVEC 24 h after the addition of ESA were determined with a real-time PCR system (DNA Engine Opticon™ 2 System, MJ Research, CA), which allows real-time quantitative detection of PCR products by measuring the increase in fluorescence caused by binding of SYBR green to double-stranded DNA. The cDNA was made using a Ready-To-Go T-Primed First-Strand Kit (Amersham Pharmacia Biotech, NJ) from the total RNA in HUVEC 24 h after the addition of ESA. The cDNA was subjected to PCR amplification using a DyNAmo 2-{2-[(3-Dimethylamino-propyl)- propylamino]-1-phenyl- 1H-chinolin-4-ylidenmethyl}-3-methyl-benzothiazol-3-ium-Kation Green qPCR kit (Finnzymes, Espoo, Finland) and gene-specific primers for VEGF-R1, VEGF-R2, PPARγ, Bax, Bcl-2 or glyceraldehyde-3-phosphate dehydrogenase. Primer pairs used for
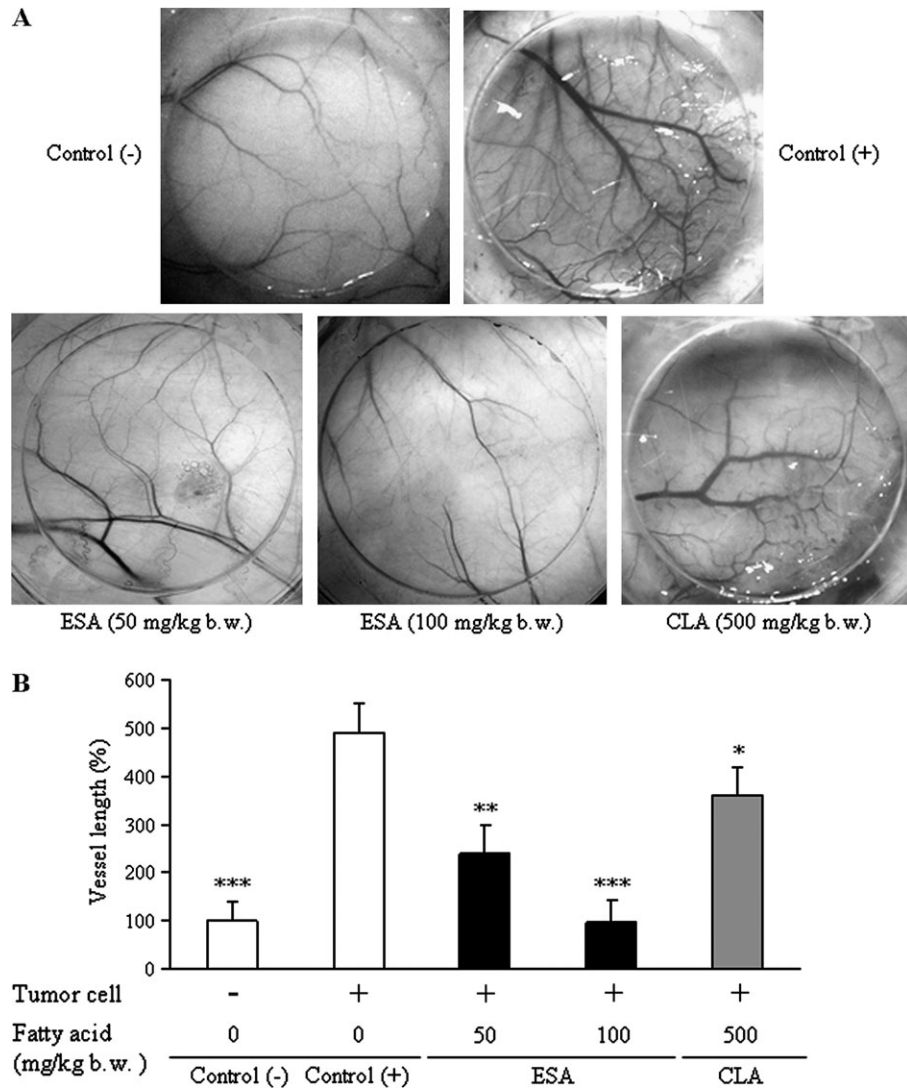
Fig. 1. Inhibitory effect of ESA on *in vivo* angiogenesis (mouse dorsal air sac assay). Chambers filled with a suspension of DLD-1 human colorectal adenocarcinoma cells were implanted subcutaneously in ICR mice. After 7 days of feeding with ESA (50 or 100 mg/kg body wt) or CLA (500 mg/kg body wt), the chambers were excised and the distribution of vessels around them was photographed. Distribution of blood vessels in chambers filled with phosphate-buffered saline and DLD-1 cell suspension in ESA- or CLA-treated mice (**A**). The distribution of blood vessels around the chambers was photographed and analyzed using Adobe Photoshop (**B**). Control mice (− or +) received chambers containing phosphate-buffered saline (−) or DLD-1 cells (+) and were administered corn oil (vehicle). Values are shown as means ± standard deviation, $n = 12$. $^{*}P < 0.05$, $^{**}P < 0.01$ and $^{***}P < 0.005$ versus control (+); b.w., body wt of mouse; −, no addition; +, addition.

VEGF-R1 were forward 5′-GTCACAGAAGAGGATGAAGGTGTCTA-3′, reverse 5′-CACAGTCCGGCACGTAGGTGATT-3′; for VEGF-R2, forward 5′-GCATCTCATCTGTTACAGC-3′, reverse 5′-CTTCATCAATCTTTACCCC-3′; for PPARγ, forward 5′-GCAGGAGCAGAGCAAAGAGGTG-3′, reverse 5′-AAATATTGCCAAGTCGCTGTCATC-3′; for Bax, forward 5′-TCATGAAGA-CAGGGGCCTTTT-3′, reverse 5′-CAATCATCCTCTGCAGCTCCA-3′; for Bcl-2, forward 5′-GGATGCCTTTGTGGAACTGT-3′, reverse 5′-AGCCTG-CAGCTTTGTTTCAT-3′; for glyceraldehyde-3-phosphate dehydrogenase, forward 5′-CCTGGCCAAGGTCATCCATG-3′, reverse 5′-GGAAGGCCATGCCAGTGAGC-3′. Real-time PCR was conducted under conditions suitable for the primers, as established in our previous studies (20,25,34). The conditions used were 95°C for 5 min, 95°C for 10 s and 59°C for 50 s >40 cycles for each gene. Melting curve analysis was performed following each reaction to confirm the presence of only a single reaction product. In addition, representative PCR products were electrophoresed on 2.0% agarose gels to verify that only a single band was present. The threshold cycle (C_T) represents the PCR cycle at which an increase in reporter fluorescence above a baseline signal could first be detected. The ratio between the glyceraldehyde-3-phosphate dehydrogenase content in standard and test samples was used to normalize the results.

Measurement of PPARγ–DNA-binding activity
HUVEC were treated for 24 h in the presence or absence of ESA (5, 10 or 20 μM), the PPARγ agonist troglitazone (10 μM) or 20 μM various fatty acids [LA, LNA, eicosapentaenoic acid, docosahexaenoic acid, 9Z11E-CLA (9Z11E) and 10E12Z-CLA (10E12Z)] in HuMedia-EG2™ medium containing VEGF (10 ng/ml). Nuclear extracts were prepared with a Nuclear Extract Kit (Active Motif, Rixensart, Belgium) according to the manufacturer's protocol, as described elsewhere (39). PPARγ–DNA-binding activity in the nuclear extracts was determined by transcription factor assay using a Trans-AM™ PPARγ Kit (Active Motif) (39).

Measurement of PPARγ transcriptional activity
HUVEC were pretreated without or with the PPARγ antagonist GW (10 μM) for 1 h before ESA (5, 10 or 20 μM) or troglitazone (10 μM) treatment and exposed ESA or troglitazone for 12 h. After treatment, nuclear extracts were collected using a NucBuster protein extraction kit (Novagen, San Diego, CA), protein concentration was determined by the method of Lowry *et al.* (40), and the PPARγ transcriptional activity was measured using NoShift™

T.Tsuzuki and **Y.Kawakami**

II PPAR Transcription Factor Assay Kit (a modified electromobility assay; Novagen) as specified by the manufacturer (41). The specificity of protein binding was established using TransCruz™ Gel Shift PPAR specific and mutant oligonucleotides (Santa Cruz Biotechnology, Santa Cruz.). Luminescence was measured by microplate luminometer (GENios).

DNA ladder (apoptosis assay)

A DNA ladder apoptosis assay was performed as described previously (20,34). HUVEC (1×10^5/ml) were treated with 20 μM ESA or 10 μM troglitazone for 24 h in HuMedia-EG2™ medium containing VEGF (10 ng/ml) and then transferred to a glass tube. Pellets were suspended in lysis buffer (5 mM Tris, 20 mM ethylenediaminetetraacetic acid, 0.5% Triton X-100 and pH 8.0) and incubated for 30 min at 4°C. After incubation, the tube was centrifuged at 15 000 r.p.m. for 20 min to separate intact chromatin from DNA fragments. Then 2 μl of RNase A (1 mg/ml) were added to the supernatant, and the mixture was incubated at 37°C for 1 h. Proteinase K (2 μl; 1 mg/ml) was then added and incubation was continued for an additional 1 h. DNA was precipitated with a mixture of 20 μl of 5M NaCl and 120 μl of 2-propanol overnight at –20°C. Following centrifugation, pellets were air dried and dissolved in 20 μl of TE buffer (10 mM Tris and 1 mM ethylenediaminetetraacetic acid, pH 7.4). Extracted DNA was electrophoresed in a 2.0% agarose gel in a mixture of 90

mM Tris, 90 mM boric acid and 2 mM ethylenediaminetetraacetic acid buffer (pH 8.4) at 100 V. Each gel was stained with ethidium bromide and photographed under UV light using the Dolphin-Chemi (Kurabo).

DNA fragmentation (apoptosis assay)

DNA fragmentation apoptosis assays were performed as described previously (13,20). HUVEC were pretreated without or with the PPARγ antagonist GW (10 μM) for 1 h before ESA (20 μM) or troglitazone (10 μM) treatment and exposed ESA or troglitazone for 24 h in HuMedia-EG2™ medium containing VEGF, as above, and then transferred to a glass tube. Lysis buffer was added and lysis was allowed to proceed for 30 min at 4°C. After incubation, the tube was centrifuged at 15 000 r.p.m. for 20 min to separate intact chromatin from DNA fragments. Lysis buffer was added to the pellets. Both pellets and supernatants were assayed for DNA content using diphenylamine. Results are expressed as the ratio of DNA amount in the supernatant to the total DNA amount recovered in both pellet and supernatant.

Statistical analysis

The Dunnett multiple comparison test or two-tailed unpaired Student's *t*-test was performed to compare findings among groups. A difference was considered to be significant at $P < 0.05$.
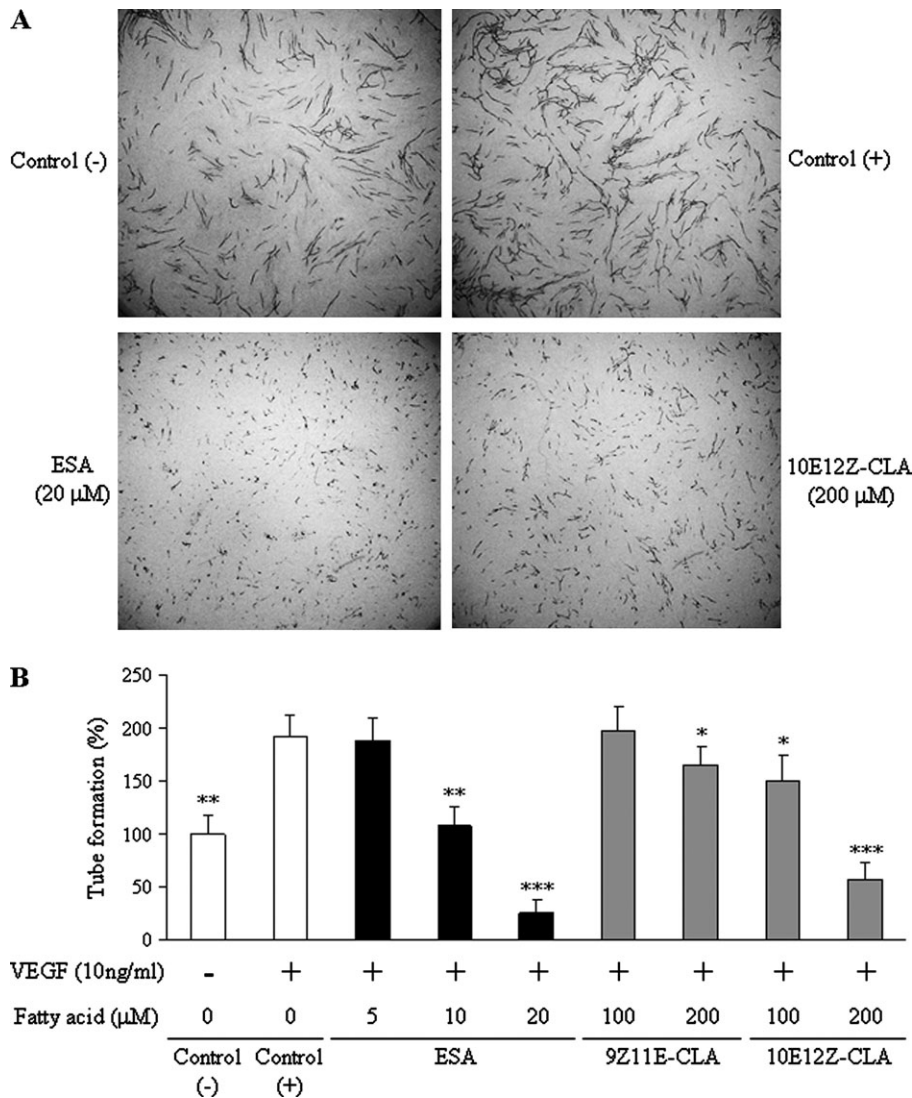

Fig. 2. Effects of ESA on tube formation by HUVEC. HUVEC cocultured with fibroblasts were incubated with medium only or with medium containing VEGF (10 ng/ml) and ESA (5, 10 or 20 μM), 9Z11E-CLA (100 or 200 μM) or 10E12Z-CLA (100 or 200 μM). After 11 days, the cells were visualized with anti-CD31 antibody and photographed (**A**). Tube formation was observed in four randomly chosen fields and the areas occupied by endothelial tubes were measured (**B**). Control cells (− or +) were cultured in medium without or with VEGF. Values are shown as means ± standard deviation, $n = 6$. *$P < 0.05$, **$P < 0.01$ and ***$P < 0.005$ versus control (+); −, no addition; +, addition.

Results

ESA inhibits tumor cell-induced angiogenesis in vivo

We first evaluated the inhibition of tumor cell-induced angiogenesis by ESA *in vivo*. Significant neovascularization from surrounding blood vessels was apparent in chambers containing DLD-1 human colorectal adenocarcinoma cells implanted in control mice (Figure 1). There were few new blood vessels in phosphate-buffered saline-filled chambers. Vessel formation was clearly suppressed in mice orally administered ESA at doses of 50 and 100 mg/kg/day in a dose-dependent manner. No effect was observed on preexisting vessels. CLA significantly suppressed vessel formation at a concentration of 500 mg/kg/day; ESA suppressed angiogenesis at doses less than one-tenth of this.

ESA inhibits VEGF-induced angiogenesis in vitro

The effect of ESA on the tubular morphogenesis of endothelial cells was next examined to determine whether ESA acts on endothelial cells directly. HUVEC and human fibroblast cocultures incubated for 11 days with 10 ng/ml VEGF showed an increased area occupied by endothelial tubes compared with cells incubated with medium only (Figure 2). ESA suppressed VEGF-induced tube formation (as measured by the length of endothelial tubes) in a concentration-dependent manner; this effect was significant at an ESA concentration of 10 μM and reached 86% suppression at an ESA concentration of 20 μM. 9Z11E-CLA and 10E12Z-CLA suppressed VEGF-induced tube formation to a significant extent at concentrations of 200 and 100 μM,

respectively. ESA suppressed angiogenesis at a concentration less than one-tenth of that at which 9Z11E-CLA and 10E12Z-CLA did so *in vitro*.

ESA inhibits VEGF-induced migration and proliferation of HUVEC

Next, the effect of ESA on the migration and proliferation of HUVEC was examined since these properties are closely related to tubular morphogenesis. A model using Boyden chamber was used to assess the impact of ESA on endothelial cell migration. In cultures supplemented with VEGF (10 ng/ml), the migration of endothelial cell was promoted (Figure 3A). ESA suppressed VEGF-induced endothelial cell migration in a concentration-dependent manner (Figure 3A); this effect was significant at an ESA concentration of 10 μM and 50% suppression was observed at a concentration of 20 μM, compared with cultures without ESA [control (+)]. 9Z11E-CLA had no influence on HUVEC migration. 10E12Z-CLA significantly suppressed VEGF-induced cell migration at a concentration of 200 μM. A WST-1 assay was used to assess the impact of ESA on endothelial cell proliferation. HUVEC were cultured in the presence or absence of VEGF and the proportion of viable cells was evaluated 72 h after the addition of ESA or CLA (Figure 3B). In cultures supplemented with VEGF (10 ng/ml), ESA almost completely reversed cell proliferation at a concentration of 10 μM. 9Z11E-CLA and 10E12Z-CLA significantly suppressed VEGF-induced cell proliferation at concentrations of 200 and 100 μM, respectively. These results show that ESA suppressed the migration and proliferation of HUVEC. And we seemed for ESA to be inhibiting the effect of VEGF.
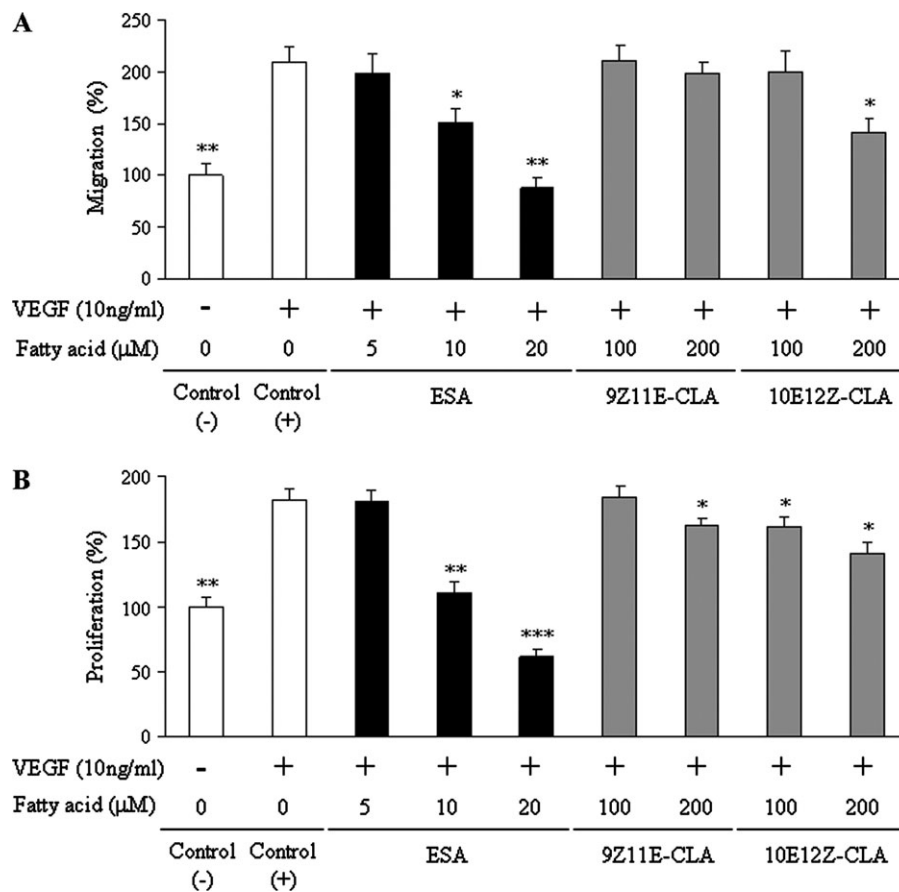

Fig. 3. Effects of ESA on HUVEC migration (**A**) and proliferation (**B**). (**A**) HUVEC were allowed to migrate for 12 h in the presence of VEGF (10 ng/ml) and ESA (5, 10 or 20 μM) or CLA (100 or 200 μM), then stained and measured. Migrating cells were determined by fluorescent enzyme-linked immunosorbent assay reader at 480/520 nm. (**B**) HUVEC were incubated in medium containing VEGF (10 ng/ml) and ESA (5, 10 or 20 μM) or CLA (100 or 200 μM) for 24 h. Numbers of viable cells were assessed in a WST-1 assay. Values are shown as means ± standard deviation, $n = 6$. $^{*}P < 0.05$, $^{**}P < 0.01$ and $^{***}P < 0.005$ versus control (+); −, no addition; +, addition.
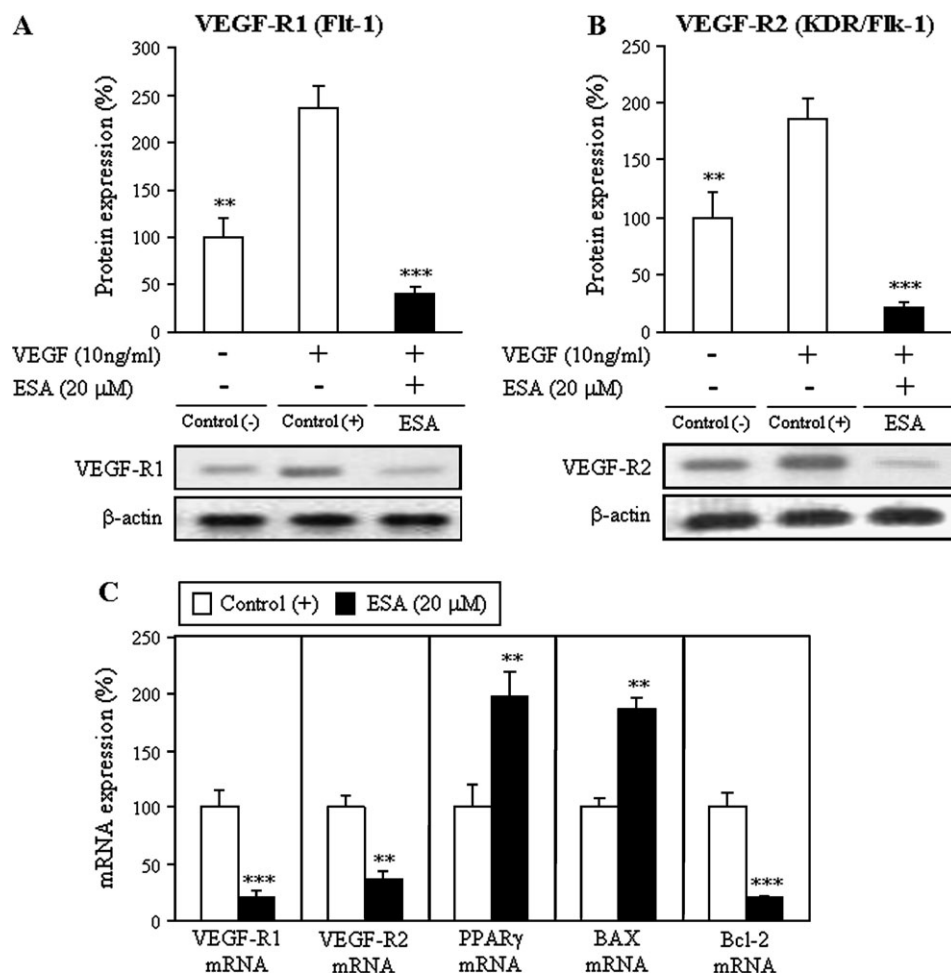
Fig. 4. Expression of VEGF-R1 (Flt1) proteins (**A**) and VEGF-R2 (KDR/Flk-1) proteins (**B**) in HUVEC treated with ESA and VEGF (10 ng/ml) compared with control cells. Expression of VEGF-R1, VEGF-R2, PPARγ, Bax and Bcl-2 mRNA in HUVEC treated with VEGF (10 ng/ml) and ESA compared with control cells (**C**). HUVEC were incubated for 24 h after treatment with 20 μM ESA and analyzed using western blotting (**A** and **B**) or a real-time quantitative RT–PCR assay (**C**). Control cells (− or +) were cultured in medium without or with VEGF. Values are shown as means ± standard deviation, $n = 6$. $^*P < 0.05$, $^{**}P < 0.01$ and $^{***}P < 0.005$ versus control (+); −, no addition; +, addition.

ESA inhibits VEGF-R1 and VEGF-R2 expression by HUVEC

We next evaluated the mechanism by which ESA inhibits angiogenesis *in vitro* by measuring the expression of well-characterized angiogenic factors, especially those associated with cell migration and proliferation such as the VEGF-R. Western blotting for VEGF-R1 (Flt1) and VEGF-R2 (KDR/Flk-1) showed that ESA at concentrations that suppressed tube formation caused downregulation of VEGF-induced VEGF-R1 and VEGF-R2 expression by HUVEC (Figure 4A and B). To examine this in greater detail, expression levels of VEGF-R1 and VEGF-R2 mRNA in HUVEC were measured using a real-time quantitative RT–PCR assay which showed that ESA at concentrations that suppressed tube formation caused downregulation of VEGF-induced VEGF-R1 and VEGF-R2 mRNA expression (Figure 4C). Since ESA is a polyunsaturated fatty acid, it was thought possible that it might function as a PPARγ ligand.

ESA activates PPARγ in HUVEC

To determine whether ESA activates PPARγ, the effect of ESA on the expression of PPARγ mRNA, the PPARγ–DNA-binding activity and the PPARγ transcriptional activity of HUVEC were examined. Expression levels of PPARγ mRNA in HUVEC were measured using a real-time quantitative RT–PCR assay which showed that ESA at concentrations that suppressed tube formation caused upregulation of PPARγ mRNA expression (Figure 4C). PPARγ–DNA-binding ac-

tivity and transcriptional activity in HUVEC were measured using a transcription factor assay kit and showed that ESA upregulated PPARγ–DNA-binding activity in a concentration-dependent manner (Figure 5). The PPARγ–DNA-binding activity induced by 20 μM ESA was comparable with that induced by 10 μM troglitazone (a known PPARγ agonist) and was very strong compared with that induced by other fatty acids of the same concentration (Figure 5A). Furthermore, to investigate whether the PPARγ transcriptional activity could be increased after ESA induction of PPARγ expression, a modified electromobility shift assay was employed to investigate the interaction between PPARγ and its responsive DNA. We found that the exposure of cells to varying concentrations of ESA for 12 h induced a dose-dependent increase of DNA binding of PPARγ (Figure 5B), suggesting enhancement of PPARγ transcriptional activity. To identify the PPARγ isoform responsible for this effect, HUVEC pretreated with the PPARγ specific inhibitor GW (10 μM, 1 h) before ESA treatment. The suppression of the DNA-binding effect indicates the major binding factor is PPARγ.

ESA induces apoptosis in HUVEC

To determine whether ESA induces apoptosis in HUVEC, Bax (an apoptosis-inducing factor) and Bcl-2 (an apoptosis-suppressing factor) mRNA expression was measured using a real-time quantitative RT–PCR assay. This showed that ESA at concentrations that
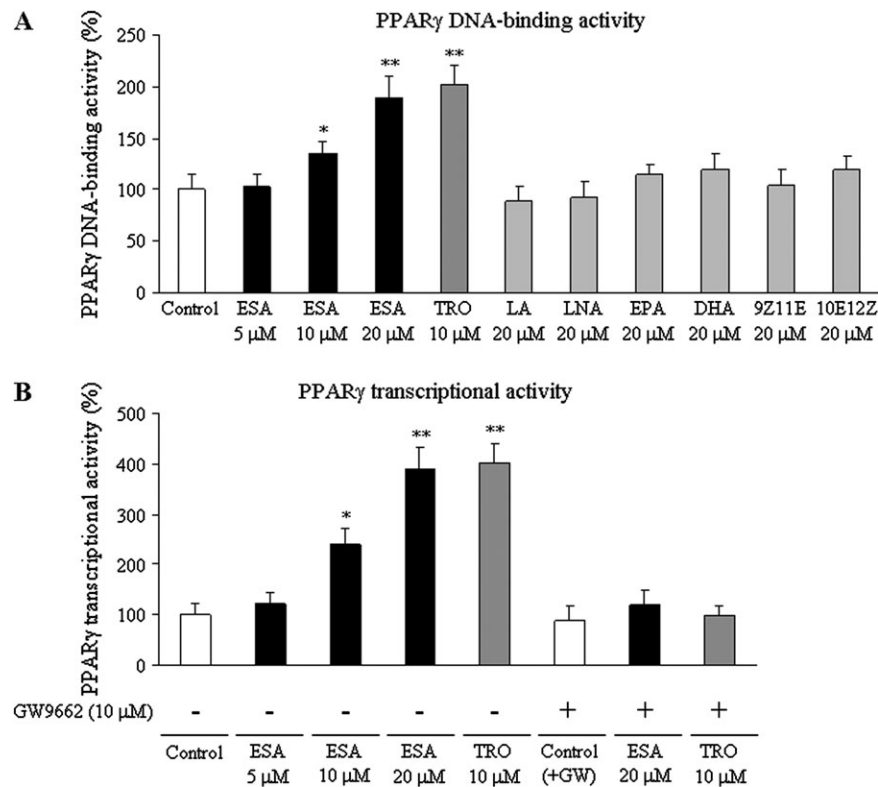
Fig. 5. ESA induced PPARγ–DNA-binding activity (**A**) and PPARγ transcriptional activity (**B**) in HUVEC treated with VEGF (10 ng/ml). HUVEC were incubated simultaneously with VEGF and ESA (5, 10 or 20 μM), the PPARγ agonist troglitazone (10 μM) or 20 μM various fatty acids [LA, LNA, eicosapentaenoic acid, docosahexaenoic acid, 9Z11E-CLA (9Z11E), and 10E12Z-CLA (10E12Z)] for 24 h. PPARγ transactivation was determined using an enzyme-linked immunosorbent assay-based transactivation assay that measured PPARγ binding to its specific consensus binding site (**A**). HUVEC were pretreated without or with the PPARγ antagonist GW (10 μM) for 1 h before ESA (5, 10 or 20 μM) or troglitazone (10 μM) treatment and exposed ESA or troglitazone for 12 h. Nuclear proteins were then extracted and aliquots containing equal amounts of protein were subjected to PPARγ transcriptional activity assay (**B**). Control cells were cultured in medium without fatty acids and troglitazone. Control cells (+GW) were cultured in medium with GW (10 μM). Values are shown as means ± standard deviation, $n = 6$. $^{*}P < 0.05$ and $^{**}P < 0.01$ versus control; −, no addition; +, addition.

suppressed tube formation upregulated BAX mRNA expression and down-regulated Bcl-2 mRNA expression (Figure 4C). The induction of apoptosis was also assessed by examining DNA fragmentation and DNA ladder generation; the results showed that ESA at concentrations that suppressed tube formation caused increased DNA fragmentation and generated a DNA ladder in HUVEC (Figure 6). Troglitazone at concentrations that suppressed tube formation also caused increased DNA fragmentation and generated a DNA ladder in HUVEC. The DNA fragmentation and DNA ladder generation induced by 20 μM ESA was comparable with that induced by 10 μM troglitazone. These phenomena were abolished by GW that was the antagonist of PPARγ. Therefore, it was shown that ESA and troglitazone suppressed angiogenesis via PPARγ.

Discussion

In this study, we have demonstrated for the first time that ESA, a conjugated linolenic acid present in tung oil, exerts antiangiogenic effects both *in vivo* and *in vitro*. In the experiments reported here, we measured tumor cell-induced angiogenesis *in vivo* and the proliferation, migration and tube formation of HUVEC using the known antiangiogenic effects of CLA (21,22) as a positive control. ESA strongly suppressed DLD-1 cell-induced angiogenesis *in vivo* compared with CLA (Figure 1), and it was considered possible that this might have resulted from ESA acting directly on DLD-1 cells. Therefore, the effect of ESA on endothelial cell tubular morphogenesis was examined to determine whether ESA acts directly on endothelial cells. DLD-1 cells are known to secrete VEGF, which induces angiogenesis (42). Angiogenesis was therefore induced using VEGF in our *in vitro*

tumor-induced angiogenesis model. ESA inhibited the formation of capillary-like networks by HUVEC (Figure 2) and moderately inhibited HUVEC proliferation and migration in a dose-dependent manner (Figure 2). The ESA concentration required for the suppression of tube formation was comparable with that required for the suppression of cell proliferation and migration, suggesting that the main effect of ESA is the suppression of HUVEC migration and proliferation. 9Z11E-CLA and 10E12Z-CLA also suppressed tube formation *in vitro*, but only at concentrations 10 times greater than ESA (Figure 2). This suggests that the conjugated double bond in ESA is important for its antiangiogenic activity; in this context, it is noteworthy that CLA exerts an antiangiogenic effect whereas LA does not (21,22). In addition, it has been understood that the conjugated triene system of ESA has strong effects compared with the conjugated diene system of CLA.

The mechanism by which ESA inhibits angiogenesis was first investigated by measuring the expression of the angiogenesis inducing agent VEGF-R. ESA was found to suppress VEGF-R expression and to inhibit VEGF-induced angiogenesis (Figure 4). PPARγ ligands have been reported to induce endothelial cell apoptosis, suppress VEGF-R expression and inhibit angiogenesis (28,33,41). Further, polyunsaturated fatty acids such as ESA have been reported to function as PPARγ ligands (33). To determine whether ESA activates PPARγ, the effects of ESA on PPARγ mRNA expression, PPARγ DNA-binding activity and the PPARγ transcriptional activity in HUVEC were examined and each was shown to be upregulated (Figures 4 and 5). ESA upregulated BAX (an apoptosis-inducing factor) mRNA expression, increased DNA fragmentation and down-regulated Bcl-2 (an apoptosis-suppressing factor) mRNA expression in HUVEC
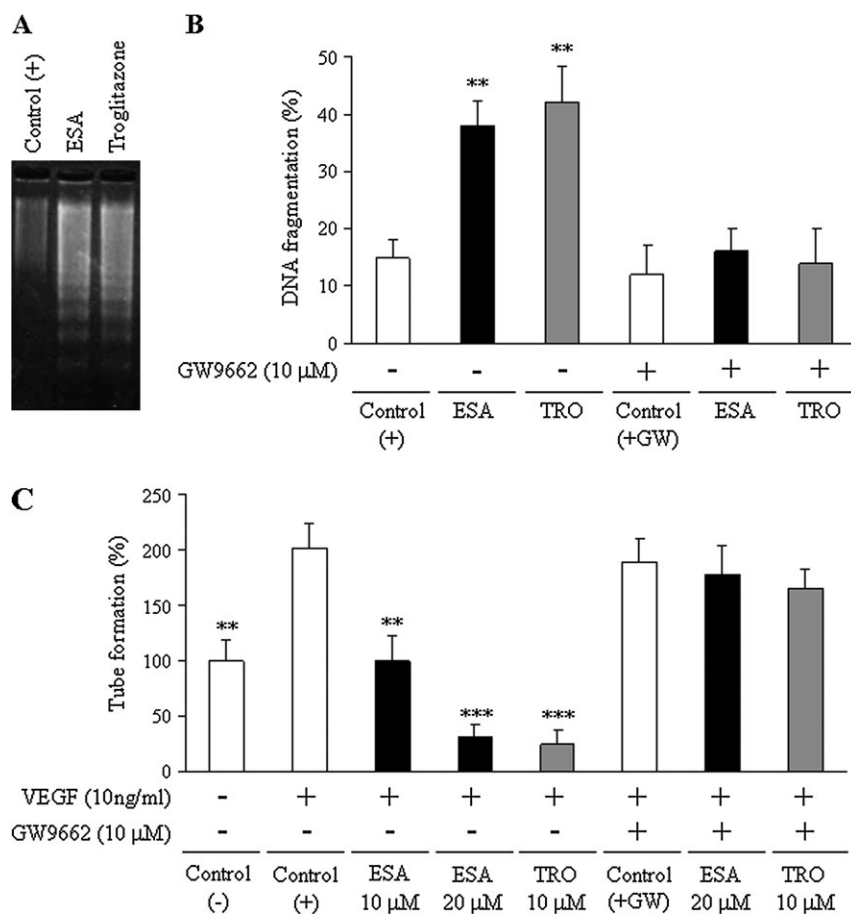
Fig. 6. DNA ladders (**A**), DNA fragmentation (**B**) and tube formation (**C**) in HUVEC treated with ESA (20 µM), troglitazone (10 µM) or GW (10 µM) and VEGF (10 ng/ml). HUVEC were incubated for 24 h after treatment with ESA or troglitazone and VEGF. DNA fragmentation agarose gel electrophoresis of low-molecular-weight DNA extracted from HUVEC (**A**). HUVEC were pretreated without or with the PPARγ antagonist GW (10 µM) for 1 h before ESA (20 µM) or troglitazone (10 µM) treatment and exposed ESA or troglitazone for 24 h. DNA fragmentation ratio of DNA extracted from HUVEC (**B**). HUVEC cocultured with fibroblasts were pretreated without or with the PPARγ antagonist GW (10 µM) for 1 h and were incubated with medium only or with medium containing VEGF (10 ng/ml) and ESA (10 or 20 µM) or troglitazone (10 µM) (**C**). After 4 days, the cells were visualized with anti-CD31 antibody and photographed. Areas occupied by endothelial tubes were measured in four randomly chosen fields. Control cells (− or +) were cultured in medium without or with VEGF. Control cells (+GW) were cultured in medium with GW (10 µM). Values are shown as means ± standard deviation, $n = 6$. $^{*}P < 0.05$, $^{**}P < 0.01$ and $^{***}P < 0.005$ versus control (+); −, no addition; +, addition.

(Figures 4 and 6). Therefore, we clarified that ESA, like troglitazone, is a PPARγ ligand, activates PPARγ, induces apoptosis in HUVEC and inhibits angiogenesis. As far as we are aware, this is the first study to demonstrate the inhibitory effect of ESA on angiogenesis.

Inhibition of angiogenesis may induce dormancy of a tumor rather than killing it, so the administration of antivascular agents may be effective in maintaining long-term remission in patients with advanced metastatic disease resistant to other types of treatment (43). Antiangiogenesis as a therapeutic concept was developed in the early 1970s. Recent data confirm that the PPARγ pathway may be a therapeutic target for numerous pathologies in which excessive angiogenesis is implicated, including cancer (29). PPARγ ligands, by inhibiting angiogenesis through their effects on the endothelium, may have clinical application in inhibiting primary tumor growth and metastasis, exerting direct and indirect antiangiogenic effects. It is also possible that multidrug-resistant tumors could be effectively targeted by antiangiogenic chemotherapy (44,45). PPARγ ligands that induce tumor cell differentiation and/or death by apoptosis may also be future therapeutic candidates, as the inhibition of angiogenesis represents one of the more promising new approaches to anticancer therapy.

Screening for compounds with antiangiogenic properties from natural sources is currently an active area of research: curcumin (46), flavonoids (47), selenium (48), N-acetylcysteine (49), vitamin D3 (50), tocotrienols (24) and several polyunsaturated fatty acids in di-

etary supplements (21,22,25,26) have all been shown to inhibit angiogenesis *in vitro* and/or *in vivo*. In this study, we have taken particular note of the properties of tung oil, a vegetable oil that contains a conjugated linolenic acid that can be prepared in bulk from a natural source. ESA is much easier to purify than CLA and has a strong antitumor effect. Hence, it is probably to be very useful, particularly since this study and our previous work have shown the safety of ESA in animals (12,15,19,20). In the Philippines and Okinawa, a region of Japan renowned for the longevity of its inhabitants, people often eat bitter gourds that contain ESA, thereby suggesting that ESA might be of significance in promoting longevity. Most CLA in nature is in the form of 9Z11E-CLA (1). However, natural sources contain minute amounts of CLA and, therefore, CLA for experimental use is generally prepared from LA by alkali isomerization. CLA prepared by alkali isomerization consists of two isomers: 9Z11E-CLA and 10E12Z-CLA. An antitumor effect of CLA prepared by alkali isomerization has been demonstrated in a number of studies, but it was recently verified in a comparative study that 9Z11E-CLA had little effect and 10E12Z-CLA, the minor isomer in nature, had a strong effect (1–6,20). This was confirmed in the present study, in which 10E12Z-CLA had a stronger tumor growth suppression effect than 9Z11E-CLA (Figures 2 and 3).

For ESA administration in humans, the dosage is important. At present, CLA is the only conjugated fatty acid that has been

investigated in humans. CLA administered to humans at a dose of 4 g/day for 9–12 weeks shows no serious side effects (7,8). The human dose equivalent to the dose given to mice in this study is <4 g/day. Therefore, the administration of ESA in humans is probable, although the effectiveness of long-term administration will need to be verified. Furthermore, the combination of conjugated fatty acids with other agents may provide an even stronger antitumor effect, even at a lower dose, and this should also be investigated. It is difficult to obtain conjugated fatty acids (including CLA) from food at an effective dose, and therefore it may be desirable to obtain conjugated fatty acids from added medicines or supplements.

Funding

Acknowledgements

References

1. Pariza,M.W. *et al*. (2001) The biologically active isomers of conjugated linoleic acid. *Prog. Lipid Res.*, **40**, 283–298.
2. Pariza,M.W. *et al*. (1985) A beef-derived mutagenesis modulator inhibits initiation of mouse epidermal tumors by 7,12-dimethylbenz[a]anthracene. *Carcinogenesis*, **6**, 591–593.
3. Ha,Y.L. *et al*. (1987) Anticarcinogens from fried ground beef: heat-altered derivatives of linoleic acid. *Carcinogenesis*, **8**, 1881–1887.
4. Ip,C. *et al*. (1994) Conjugated linoleic acid suppresses mammary carcinogenesis and proliferative activity of the mammary gland in the rat. *Cancer Res.*, **54**, 1212–1215.
5. Ip,C. *et al*. (1997) Retention of conjugated linoleic acid in the mammary gland is associated with tumor inhibition during the postinitiation phase of carcinogenesis. *Carcinogenesis*, **18**, 755–759.
6. Hubbard,N.E. *et al*. (2000) Reduction of murine mammary tumor metastasis by conjugated linoleic acid. *Cancer Lett.*, **150**, 93–100.
7. Larsen,T.M. *et al*. (2003) Efficacy and safety of dietary supplements containing CLA for the treatment of obesity: evidence from animal and human studies. *J. Lipid Res.*, **44**, 2234–2241.
8. Gaullier,J.M. *et al*. (2005) Supplementation with conjugated linoleic acid for 24 months is well tolerated by and reduces body fat mass in healthy, overweight humans. *J. Nutr.*, **135**, 778–784.
9. Badami,R.C. *et al*. (1980) Structure and occurrence of unusual fatty acids in minor seed oils. *Prog. Lipid Res.*, **19**, 119–153.
10. Lopez,A. *et al*. (1987) Two new eicosapentaenoic acids from the temperate red seaweed Ptilota filicina J. Agardh. *Lipids*, **22**, 190–194.
11. Mikhailova,M.V. *et al*. (1995) Structure and biosynthesis of novel conjugated polyene fatty acids from the marine green alga *Anadyomene stellata*. *Lipids*, **30**, 583–589.
12. Tsuzuki,T. *et al*. (2003) A metabolic conversion of 9,11,13-eleostearic acid (18:3) to 9,11-conjugated linoleic acid (18:2) in the rat. *J. Nutr. Sci. Vitaminol.*, **49**, 195–200.
13. Tsuzuki,T. *et al*. (2004) Conjugated eicosapentaenoic acid inhibits transplanted tumor growth via membrane lipid peroxidation in nude mice. *J. Nutr.*, **134**, 1162–1166.
14. Tsuzuki,T. *et al*. (2004) Oxidation rate of conjugated linoleic acid and conjugated linolenic acid is slowed by triacylglycerol esterification and α-tocopherol. *Lipids*, **39**, 475–480.
15. Tsuzuki,T. *et al*. (2004) α-Eleostearic acid (9Z11E13E-18:3) is quickly converted to conjugated linoleic acid (9Z11E-18:2) in rats. *J. Nutr.*, **134**, 2634–2639.
16. Tsuzuki,T. *et al*. (2005) Synthesis of the conjugated trienes 5E,7E,9E,14-Z,17Z-eicosapentaenoic acid and 5Z,7E,9E,14Z,17Z-eicosapentaenoic acid, and their induction of apoptosis in DLD-1 colorectal adenocarcinoma human cells. *Lipids*, **40**, 147–154.
17. Tsuzuki,T. *et al*. (2005) Intake of conjugated eicosapentaenoic acid suppresses lipid accumulation of liver and epididymal adipose tissue in rats. *Lipids*, **40**, 1117–1123.
18. Tsuzuki,T. *et al*. (2006) Conjugated docosahexaenoic acid inhibits lipid accumulation in rats. *J. Nutr. Biochem.*, **17**, 518–524.
19. Tsuzuki,T. *et al*. (2006) Conjugated linolenic acid is slowly absorbed in rat intestine, but quickly converted to conjugated linoleic acid. *J. Nutr.*, **136**, 2153–2159.
20. Tsuzuki,T. *et al*. (2004) Tumor growth suppression by α-eleostearic acid, a linolenic acid isomer with a conjugated triene system, via lipid peroxidation. *Carcinogenesis*, **25**, 1417–1425.
21. Masso-Welch,P.A. *et al*. (2002) Inhibition of angiogenesis by the cancer chemopreventive agent conjugated linoleic acid. *Cancer Res.*, **62**, 4383–4389.
22. Masso-Welch,P.A. *et al*. (2004) Isomers of conjugated linoleic acid differ in their effects on angiogenesis and survival of mouse mammary adipose vasculature. *J. Nutr.*, **134**, 299–307.
23. Kim,K.J. *et al*. (1993) Inhibition of vascular endothelial growth factor-induced angiogenesis suppresses tumour growth *in vivo*. *Nature*, **362**, 841–844.
24. Inokuchi,H. *et al*. (2003) Anti-angiogenic activity of tocotrienol. *Biosci. Biotechnol. Biochem.*, **67**, 1623–1627.
25. Tsuzuki,T. *et al*. (2007) Conjugated eicosapentaenoic acid inhibits the VEGF-induced angiogenesis by suppressing the migration of human umbilical vein endothelial cell. *J. Nutr.*, **137**, 641–646.
26. Tsuzuki,T. *et al*. (2007) Anti-angiogenic effects of conjugated docosahexaenoic acid *in vitro* and *in vivo*. *Biosci. Biotechnol. Biochem.*, **71**, 1902–1910.
27. Folkman,J. *et al*. (1992) Angiogenesis. *J. Biol. Chem.*, **267**, 10931–10934.
28. Xin,X. *et al*. (1999) Peroxisome proliferator-activated receptor gamma ligands are potent inhibitors of angiogenesis *in vitro* and *in vivo*. *J. Biol. Chem.*, **274**, 9116–9121.
29. Panigrahy,D. *et al*. (2002) PPARγ ligands inhibit primary tumor growth and metastasis by inhibiting angiogenesis. *J. Clin. Invest.*, **110**, 923–932.
30. Panigrahy,D. *et al*. (2005) PPARγ as a therapeutic target for tumor angiogenesis and metastasis. *Cancer Biol. Ther.*, **4**, 687–693.
31. Kim,K.Y. *et al*. (2006) Antiangiogenic effect of rosiglitazone is mediated via peroxisome proliferator-activated receptor γ-activated maxi-K channel opening in human umbilical vein endothelial cells. *J. Biol. Chem.*, **281**, 13503–13512.
32. Schoonjans,K. *et al*. (1997) Peroxisome proliferator-activated receptors, orphans with ligands and functions. *Curr. Opin. Lipidol.*, **8**, 159–166.
33. Margeli,A. *et al*. (2003) Peroxisome proliferator activated receptor-γ (PPAR-γ) ligands and angiogenesis. *Angiogenesis*, **6**, 165–169.
34. Tsuzuki,T. *et al*. (2007) Conjugated EPA activates mutant p53 via lipid peroxidation and induces p53-dependent apoptosis in DLD-1 colorectal adenocarcinoma human cells. *Biochim. Biophys. Acta*, **1771**, 20–30.
35. Oak,J.-H. *et al*. (2003) Amadori-glycated phosphatidylethanolamine induces angiogenic differentiations in cultured human umbilical vein endothelial cells. *FEBS Lett.*, **555**, 419–423.
36. Igarashi,M. *et al*. (2004) Recommended methods of fatty acid methylester preparation for conjugated dienes and trienes in food and biological samples. *J. Nutr. Sci. Vitaminol.*, **50**, 121–128.
37. Tsuzuki,T. *et al*. (2007) Slow absorption of conjugated linoleic acid in rat intestines, and similar absorption rates of 9c,11t-conjugated linoleic acid and 10t,12c-conjugated linoleic acid. *Biosci. Biotechnol. Biochem.*, **71**, 2034–2040.
38. Yonekura,K. *et al*. (1999) UFT and its metabolites inhibit the angiogenesis induced by murine renal cell carcinoma, as determined by a dorsal air sac assay in mice. *Clin. Cancer Res.*, **5**, 2185–2191.
39. Ringseis,R. *et al*. (2006) CLA isomers inhibit TNFα-induced eicosanoid release from human vascular smooth muscle cells via a PPARγ ligand-like action. *Biochim. Biophys. Acta*, **1760**, 290–300.
40. Lowry,O.H. *et al*. (1951) Protein measurement with the Folin phenol reagent. *J. Biol. Chem.*, **193**, 265–275.
41. Ho,T.-C. *et al*. (2007) PEDF induces p53-mediated apoptosis through PPAR gamma signaling in human umbilical vein endothelial cells. *Cardiovasc. Res.*, **76**, 213–223.
42. Hellmuth,M. *et al*. (2004) Nitric oxide differentially regulates pro- and anti-angiogenic markers in DLD-1 colon carcinoma cells. *FEBS Lett.*, **563**, 98–102.
43. Hayes,A.J. *et al*. (1999) Antivascular therapy: a new approach to cancer treatment. *BMJ*, **318**, 853–856.
44. Browder,T. *et al*. (2000) Antiangiogenic scheduling of chemotherapy improves efficacy against experimental drug-resistant cancer. *Cancer Res.*, **60**, 1878–1886.
45. Klement,G. *et al*. (2000) Continuous low-dose therapy with vinblastine and VEGF receptor-2 antibody induces sustained tumor regression without overt toxicity. *J. Clin. Invest.*, **105**, R15–R24.

46. Thaloor,D. *et al.* (1998) Inhibition of angiogenic differentiation of human umbilical vein endothelial cells by curcumin. *Cell Growth Differ.*, **9**, 305–312.
47. Cao,Y. *et al.* (1999) Angiogenesis inhibited by drinking tea. *Nature*, **398**, 381.
48. Jiang,C. *et al.* (1999) Selenium-induced inhibition of angiogenesis in mammary cancer at chemopreventive levels of intake. *Mol. Carcinog.*, **26**, 213–25.
49. Cai,T. *et al.* (1999) N-acetylcysteine inhibits endothelial cell invasion and angiogenesis. *Lab. Invest.*, **79**, 1151–1159.
50. Mantell,D.J. *et al.* (2000) 1α, 25-Dihydroxyvitamin D3 inhibits angiogenesis *in vitro* and *in vivo*. *Circ. Res.*, **87**, 214–220.